

# Design of a Device and Procedure for Characterizing the Response of the Pediatric Thorax Utilizing Nonparametric System Identification Techniques

K. Icke<sup>1</sup>, K. Moorhouse PhD<sup>2</sup>, J. Bolte IV PhD<sup>1</sup>

<sup>1</sup>The Ohio State University, <sup>2</sup>National Highway Traffic Safety Administration-Vehicle Research and Test Center

## Introduction

A 1994 epidemiology study of the National Pediatric Trauma Registry (NPTR) determined that injuries to the thorax pose a risk of fatality that is second only to head injuries in children [1]. Motor vehicle accidents are the leading cause of mortality and injury due to head and thoracic trauma in children 1 year and older [1, 2]. In an effort to protect child occupants, passenger restraint systems originally designed for adults have been adapted to protect children. Being that the clavicle and thorax are the only bony structures of the upper body to interact with seatbelts in frontal crash scenarios (as demonstrated in Figure 1), the response of the thorax in motor vehicle accidents helps dictate the position and kinematics of the spine, neck, and head. The effectiveness of these child restraint systems in preventing injury is evaluated using anthropomorphic test devices (ATDs) representative of children's stature and mass.

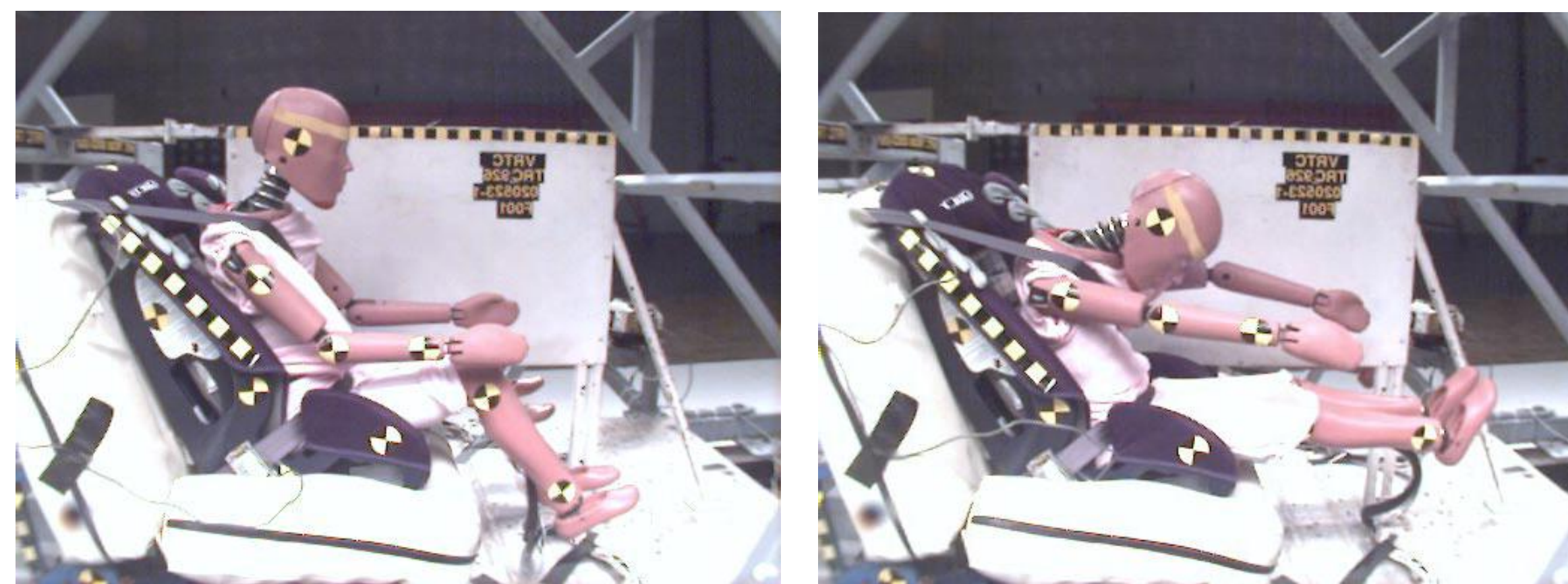


Figure 1: 10YO Child ATD Proper Restraint Frontal Loading, NHTSA.

However, the design of the biofidelic response of the child ATD is based largely on scaled down adult post mortem human subject (PMHS) data and testing with animal surrogates. The lack of mineralization of pediatric bones results in material properties that are weaker, more compliant, and less tough than those seen in skeletally mature adult bones. Figure 2 illustrates the difference in geometry of the adult and pediatric thorax, in which the pediatric ribs are more horizontal, the sternum is more superior, and the overall shape is more narrow and less flat [2].

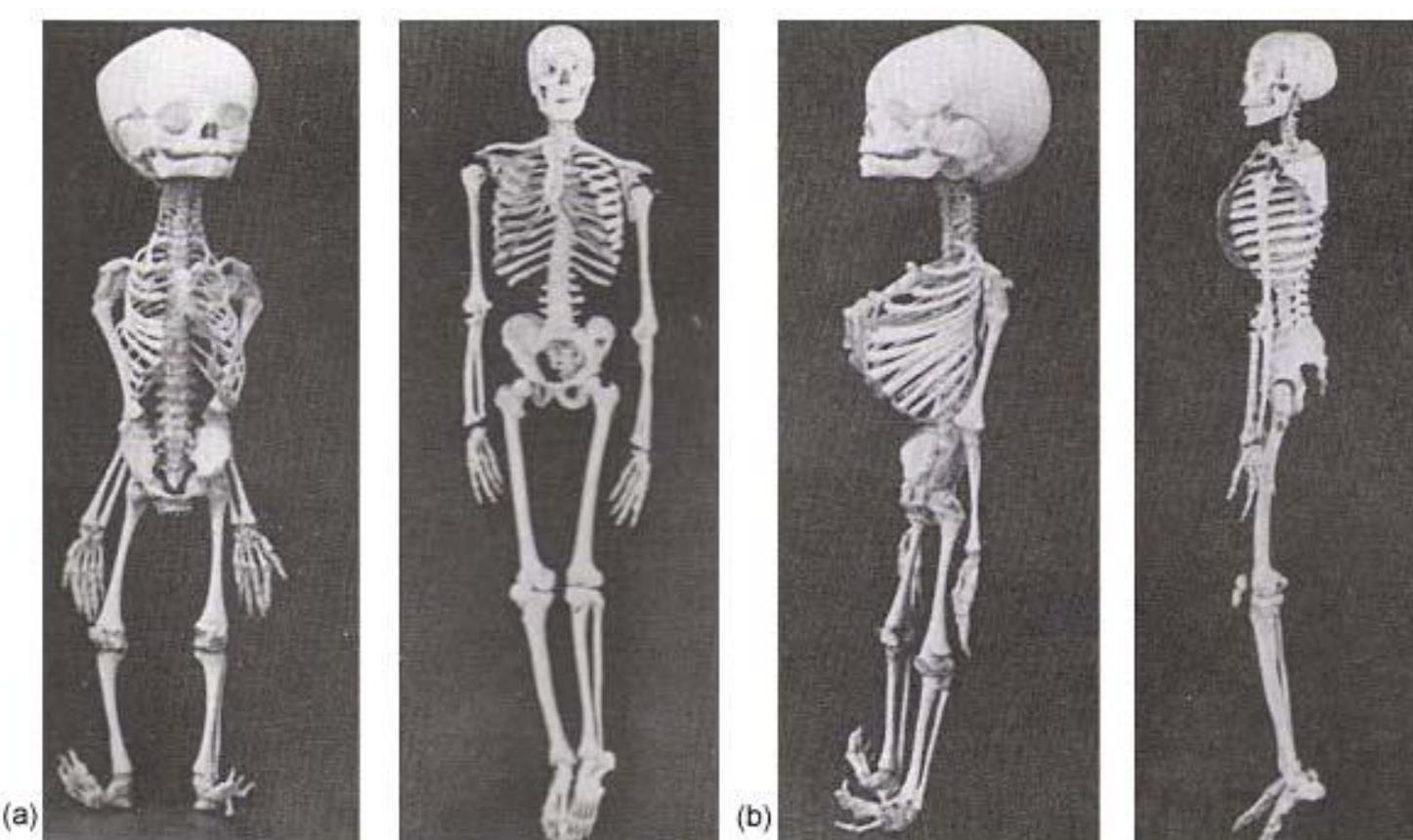


Figure 2: Comparison of Neonate and Adult Human Skeleton, Franklyn 2007.

## Objectives

➤ Design a procedure utilizing nonparametric system identification techniques to characterize the response of the adult and pediatric thorax to compressive loading in a non-injurious manner that is relevant to improving safety in motor vehicle accidents.

➤ Design and build a test device capable of loading the anterior of the thorax with small repeated perturbations in accordance with nonparametric system identification techniques that have been previously utilized to characterize nonlinear biological systems [3, 4, 5]. The fixture should be robust enough for adult thoraxes and versatile enough for pediatric thoraxes.

- Cooper, A., B. Barlow, et al. (1994). "Mortality and truncl injury: the pediatric perspective." *Journal of Pediatric Surgery* 29(1): 33.
- Franklyn, M. (2007). "Pediatric Material Properties: A Review of Human Child and Animal Surrogates." *Critical reviews in bioengineering* 35(3/4): 197.
- Hunter, I. W. and R. E. Kearney (1982). "Dynamics of human ankle stiffness: variation with mean ankle torque." *Journal of Biomechanics* 15(10): 747.
- Kearney, R. E. and I. W. Hunter (1990). "System identification of human joint dynamics." *CRC Critical Reviews in Biomedical Engineering* 18(1): 55.
- Moorhouse, K. M. and K. P. Granata (2005). "Trunk stiffness and dynamics during active extension exertions." *Journal of Biomechanics* 38(10): 2000-2007.
- Kent, R., D. Lesley, et al. (2004). "Thoracic response to dynamic, non-impact loading from a hub, distributed belt, diagonal belt, and double diagonal belts." *Stapp Car Crash Journal* 48: 495.

## Procedure

System identification is a mathematical tool used to model a dynamic system based only on measured inputs and outputs. By applying small, step-function perturbation inputs to a nonlinear system, system properties can be obtained on a linear dynamic "piece" or operating point ( $\lambda$ ) of the system. These pieces can then be compiled quasi-linearly into an overall nonlinear dynamic model of the system. In this study 10 mm input displacement perturbations will be applied to the thorax at varying levels of initial thoracic compression and perturbation speeds, each of which represent a particular operating point ( $\lambda$ ) as shown in Table I. The resultant posterior reaction forces of the thorax will be measured as the system output. The force is measured at the posterior of the thorax to eliminate the inertial component of reaction force due to accelerating the mass of the anterior thorax [6]. The only contributions to the reaction force measured at the posterior of the thorax are due to the viscous and elastic components of the thorax.

$$c_{xy}(i) = \Delta t \sum_{j=M_1}^{M_2} h(j)c_{xx}(i-j)$$

$c_{xx}$  = Autocorrelation of Input Deflection  
 $c_{xy}$  = Cross-correlation of Input Deflection/Output Force  
 $h$  = Impulse Response Function (IRF)

Figure 3: Convolution Integral Equation.

Table I: Pediatric Test Matrix.

Level of Initial Chest Deflection (%)	Perturbation Velocity (m/s)			
	Amplitude: 10mm			
8	.5	1.5	2.5	
13	.5	1.5	2.5	
18	.5	1.5	2.5	
30	.5	1.5	2.5	
40	.5	1.5	2.5	

Figure 3 shows the discrete version of the time-domain convolution integral often employed for nonparametric system identification of LTI (Linear Time-Invariant) systems (see Assumptions below). In this equation the output is described by the impulse response function (IRF) convolved with the input. Expressing the integral in terms of the input autocorrelation function and the input/output cross-correlation function drastically reduces the effect of measurement noise. Solving for the IRF (i.e., deconvolution) allows for the output of the system to be determined for any given input. The IRF is typically represented nonparametrically as a curve defining the system dynamics, and then system characteristics such as stiffness and damping can be obtained at each operating point by parameterizing the curve using an appropriate model.

### Assumptions

- 1) Causal - The system output depends on past/current inputs but not on future inputs
- 2) Linear - The system is linear so it obeys the rules of scalability and additivity. Although the thorax is a nonlinear system, the use of sufficiently small input displacement perturbations allows for the assumption that the system is operating within a "linear range."
- 3) Time-Invariant - The relationship between the system input and output does not depend on absolute time. Linear time-invariant (LTI) systems obey both assumptions 2) and 3).
- 4) Nonparametric - Underlying dynamics and system structure/order are unknown (e.g., pediatric thorax). The IRF can be found in the form of a curve and then parameterized.

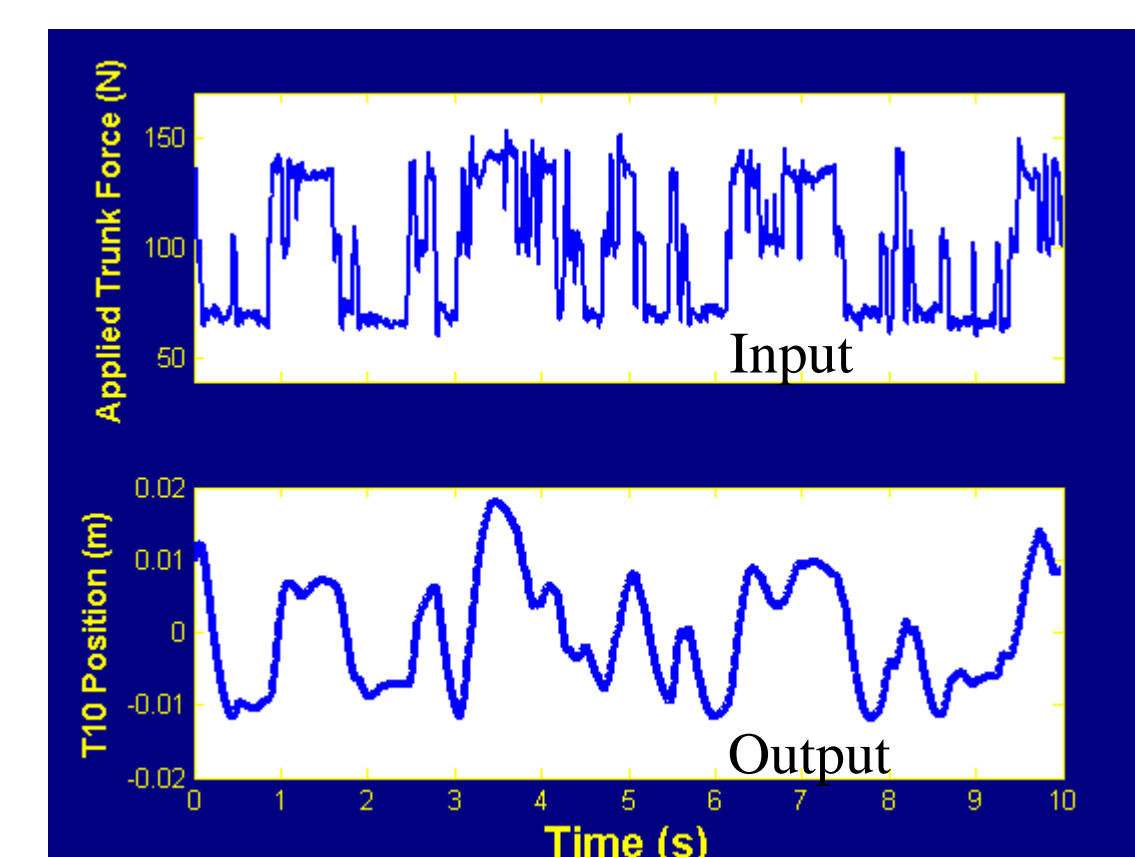


Figure 4: Example of Input and Output Sequences (Moorhouse 2005)

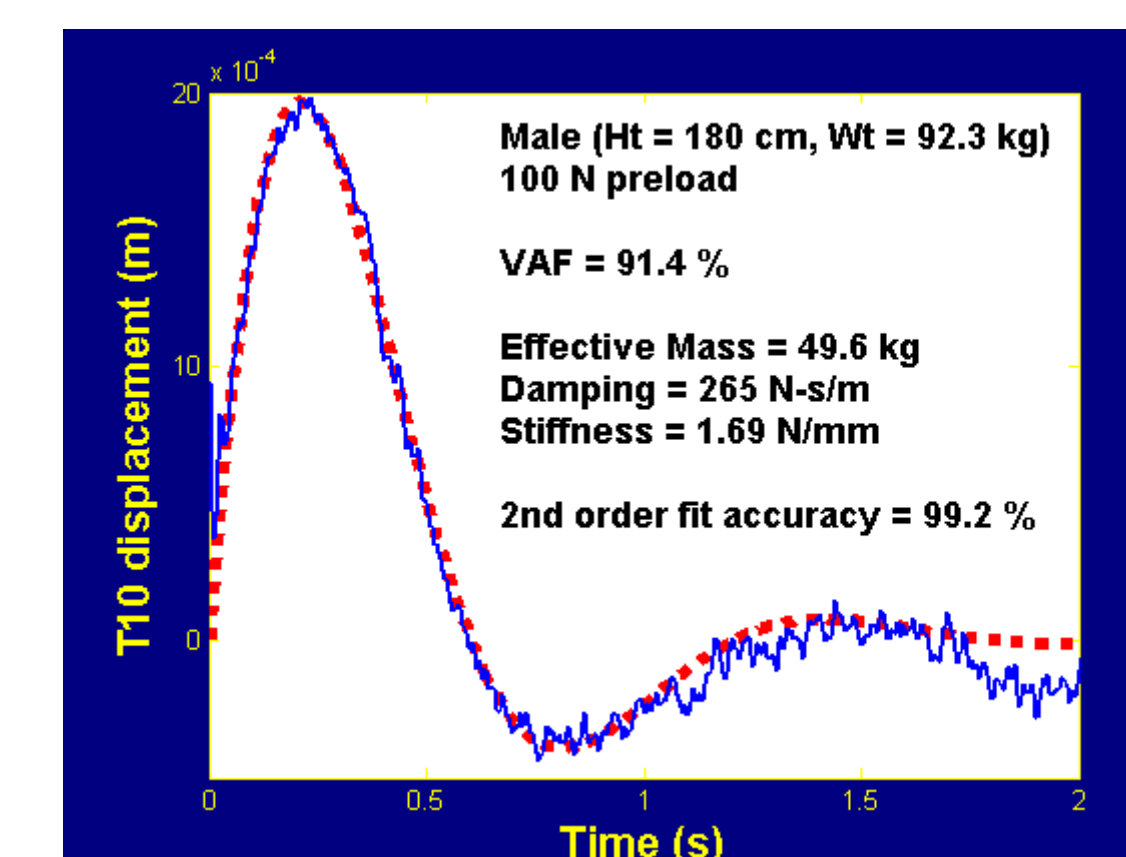


Figure 5: Example of Resulting Parameterized IRF (Moorhouse 2005)

As an example of nonparametric system identification, Figure 4 shows system input and output sequences from Moorhouse (2005), and Figure 5 shows the resulting IRF which was then parameterized using an under-damped linear second-order model (Figure 6).

$$H(s) = \frac{1}{ms^2 + bs + k}$$

Figure 6: Compliance Model.

$m$  = effective mass  
 $b$  = effective damping  
 $k$  = effective stiffness  
 $H$  = IRF

## Test Device

The test device is comprised of a 3 horsepower high inertia vector motor ZDM3764T (Baldor Electric Company), VS1GV 120Vac single phase input drive (Baldor Electric Company), a 5.76:1 ratio parallel shaft speed reducer FT77GAM213 (SEW Eurodrive Inc.), a high inertia sheave 6C300J used as a flywheel (Browning), a custom cam, custom pushrod with loading carriage, and an adjustable seat fixture. A maximum perturbation velocity of 2.5 m/s was chosen based on the compression velocity of the Hybrid III 50<sup>th</sup> male ATD in a New Car Assessment Program (NCAP) 48 km/h test. The energy storing flywheel allows the device the capability of applying a sequence of the 10 mm

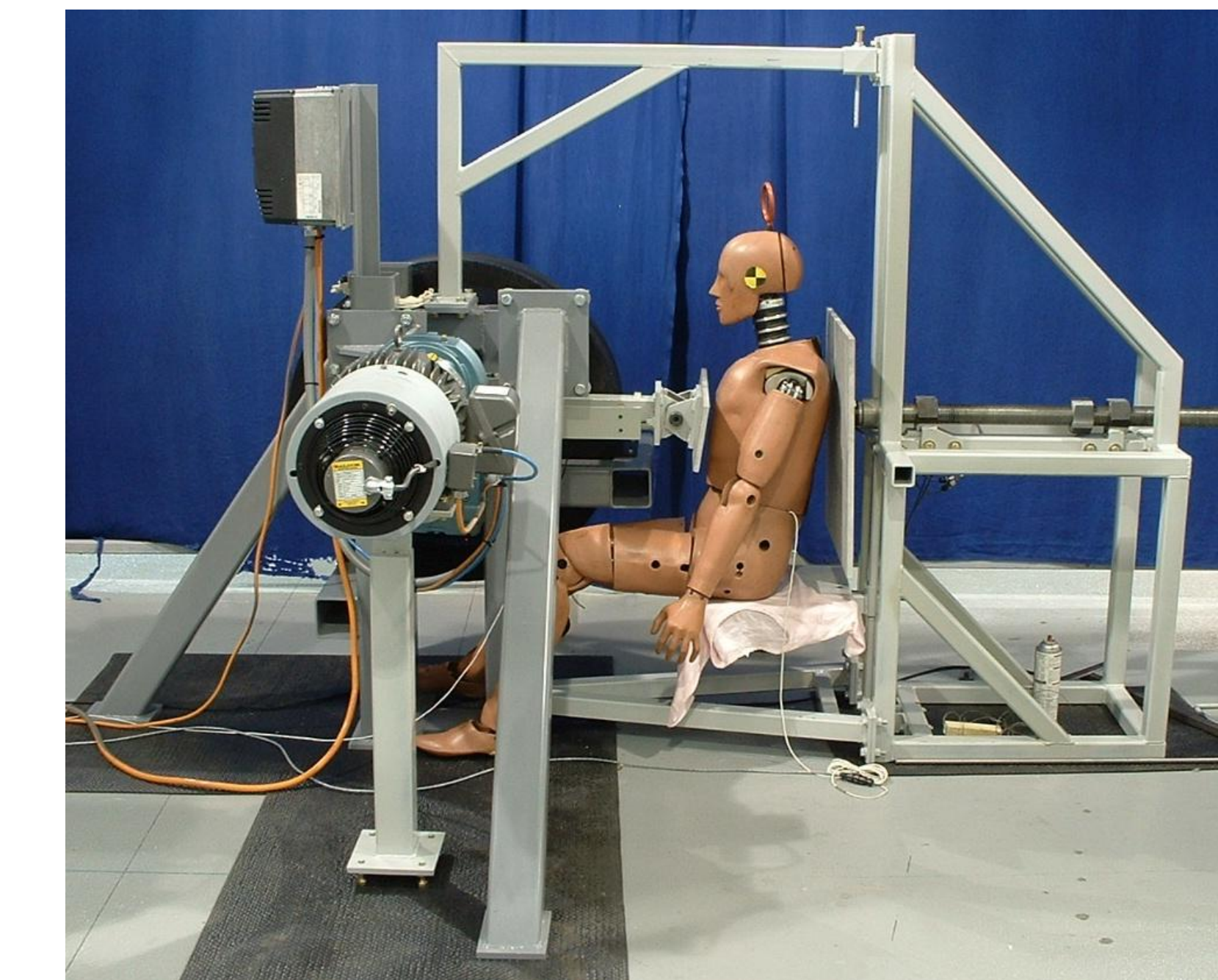


Figure 7: Thorax Test Apparatus.

compression perturbations to the thorax for 10 seconds. Thoracic response forces are collected at the posterior of the thorax via a load cell attached to the seatback. A single-pivot wide plate was chosen as the loading plate because it helps to eliminate the confounding variables seen with belt loading, such as thoracic squeeze and the belt's tendency to move superiorly during testing. The plate will not load the clavicle as a belt would. Relative-size loading is also possible with different size plates. The plate will load from the manubrium superiorly to the xiphoid process inferiorly.

## Discussion

Two Hybrid III trials and an adult PMHS trial have been completed to-date. Figure 8 shows the displacement time history for two of the Hybrid III tests. It should be noted that the original cam used in these tests produced a 12.5 mm perturbation magnitude. While the results from the first three trials were not ideal, they are promising. The input displacement perturbations exhibited an overshoot effect beyond the 12.5 mm perturbation magnitude in the high rate tests due to the large inertia of the moving parts, as seen in the red line in Figure 8. Improvements to the device are currently being implemented to eliminate this condition.

Once completed, an additional Hybrid III trial will be performed followed by another PMHS trial. Upon successful completion of these two trials the adult PMHS pilot study will commence, followed by the pediatric PMHS study. In this study a new procedure for characterizing the biofidelic response of the pediatric thorax is being developed. Utilization of nonparametric system identification techniques is a novel approach for this task and development is proceeding well.

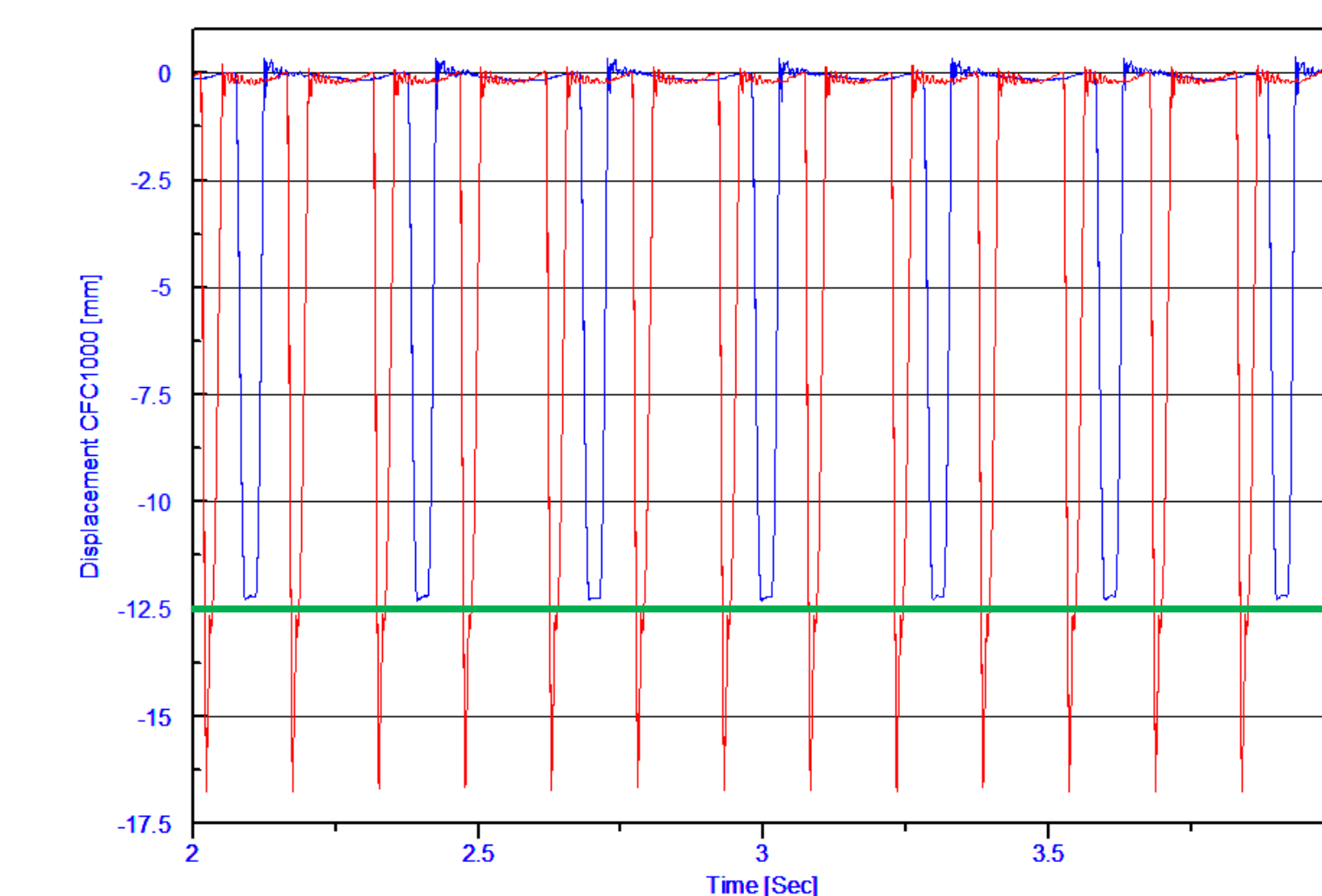


Figure 8: Hybrid III Displacement Time History: 1.3 m/s, 15% Initial Chest Compression-Blue, 2.9 m/s, 5% Initial Chest Compression-Red.